IEEE Access
Multidisciplinary | Rapid Review | Open Access Journal

Received May 27, 2019, accepted May 31, 2019, date of publication June 5, 2019, date of current version June 19, 2019.

*Digital Object Identifier 10.1109/ACCESS.2019.2921105*

# An Improved Coulomb Counting Approach Based on Numerical Iteration for SOC Estimation With Real-Time Error Correction Ability

**LIANGZONG HE, (Member, IEEE), AND DONG GUO**
Electrical Engineering Department, University of Xiamen, Xiamen 361012, China

Corresponding author: Dong Guo (xmuelemec@foxmail.com)

This work was supported in part by the Fujian Province Outstanding Youth Fund under Grant 2018J06016, in part by the Natural Science Foundation of China under Grant 61671400, and in part by the Xiamen University Nanqiang Young Top Talents Program.

**ABSTRACT** The coulomb counting (CC) approach is widely used in SOC estimation due to its simplicity and low calculation cost. However, in practical applications, the lack of error correction ability limits its accuracy due to the measured noise in the practical occasion. To address the issue, an improved CC (ICC) approach based on numerical iteration is proposed in this paper. In the proposed approach, a battery model based on a 2nd-order, *RC* circuit is first formulated to determine the *SOC-OCV* curve, *R-OCV* curve, and inner parameters. In the model, the slow dynamic and fast dynamic voltages are described separately, and are utilized for battery state assessment. Then, the SOC will be estimated by the CC approach at the unsteady state but through a numerical iteration approach at steady state. Consequently, the accumulative SOC error from the CC approach will be corrected when the numerical iteration approach is applied. Furthermore, a compensation coefficient is employed into the CC approach to reduce the error accumulation rate. Hence, the proposed ICC approach could make full use of the advantages of conventional CC in low computational demand and numerical iteration approach in error correction. Finally, an experiment platform was built, where two kinds of current sensors with different measuring accuracy were employed to simulate the measured current with and without noise, respectively. The experimental results suggest that the accumulative SOC error can be corrected in real-time and the SOC error is reduced to 1%. The error accumulation rate of SOC is effectively reduced compared with traditional CC approach, simultaneously, more than 90% of the calculation time can be reduced compared with EKF.

**INDEX TERMS** Improved coulomb counting (ICC), state of charge (SOC), accumulative error correction, numerical iteration, error accumulation rate.

## I. INTRODUCTION

To cut fossil energy consumption and mitigate the greenhouse effect, electric vehicle (EV) has been widely concerned. Battery system, as the energy provider in the EV, requires a battery management system (BMS) to ensure its safe operation [1]. Both over-charging and over-discharging will reduce the lifespan of the battery system or even lead to serious security accidents. Therefore, monitoring the state of charge (SOC), which is defined as the percentage of residual charge, has become one of the key tasks of the BMS. However, due to the complex electro-chemical behavior in a battery, estimating the exact SOC for a battery is extremely difficult in practice. Hence, the only available way is to perform an estimation of the SOC based on the measurable external parameters of the battery, such as current and voltage [2], [3].

The Coulomb Counting (CC) approach and open-circuit voltage (OCV) approach are the conventional methods to estimate SOC [4]. Ideally, CC approach could obtain relatively accurate SOC. However, in practice, there will be a large accumulated error due to the unavoidable measured noise and the lack of error correction ability. An enhanced CC approach has been proposed to improve the SOC accuracy, but the error is impossible to be eliminated fundamentally [5]. As to the OCV method, the relationship curve between SOC and battery OCV is usually applied for SOC estimation.

The associate editor coordinating the review of this manuscript and approving it for publication was Jin Sha.

Nevertheless, the OCV can be unavailable online due to the internal resistance and polarization phenomena of the battery. All in all, accurate SOC estimation online is still in suspense.

With the galloping progress of computer and artificial intelligence, intelligent algorithms such as support vector machine (SVM) and neural network (NN) are extensively concerned in SOC estimation. Without the need of detailed physical information of a battery, these algorithms explore the relationship between SOC and measured variables such as terminal voltage, current and temperature by historical data [6]–[10]. However, large amounts of historical data are required for net-training, resulting in time consuming and difficulty for implementation [3].

Model-based SOC estimation algorithms are another hot topic for SOC estimation [11]–[33]. In these algorithms, OCV is calculated based on the battery model, and then the SOC values obtained by OCV and CC are fused together using a weight coefficient. Compared with CC, error elimination ability is obtained. In general, model-based algorithms, such as EKF, UKF and H infinite filters [11], perform high accuracy and excellent stability if the battery model is ideal. However, model error can hardly be avoided in practice due to the complex chemical reaction in the battery and the noise [3], [12], even through numerous models have been proposed [13]–[24], such as the nth Thevenin model [13], multi-time scale model [14]–[16] and real-time updated model [17], [18].

To decrease the influence caused by model error, many information processing technologies are developed. The adaptive EKF can update the process and measured noise covariance in real-time [25]–[27]. The wavelet analysis technology has been employed to preprocess the measured data, which contain strong noise [28]. Algorithms using multiple filters and information fusion technologies have also been presented to improve the accuracy [29]–[33]. In these algorithms, more factors such as state of health (SOH) and models differences are considered. However, additional technologies result in the increase of calculation cost and implementation difficulty [9], [28].

In order to solve the contradiction between SOC accuracy and calculation cost, the ICC approach based on numerical iteration is proposed, where the battery model based on a 2nd-order RC circuit is built firstly with *SOC-OCV* curve, *R-OCV* curve and inner parameters identified offline. Then, the SOC is estimated by the CC approach in the unsteady state of the battery but by a numerical iteration approach in the steady state. Consequently, the accumulated SOC error from the CC approach can be corrected through the numerical iteration approach. Furthermore, a compensation coefficient is employed into CC approach to reduce the error accumulation rate. Hence, the proposed ICC approach could make full use of the advantage of conventional CC in the calculation rate and the numerical iteration approach in error correction.

This paper is organized as follows: In Section II, the 2nd-order RC model of the battery is introduced and identified. The principle of the proposed ICC approach is described in Section III. Experimental results are presented and discussed in Section IV. Finally, a brief conclusion is given in Section V.

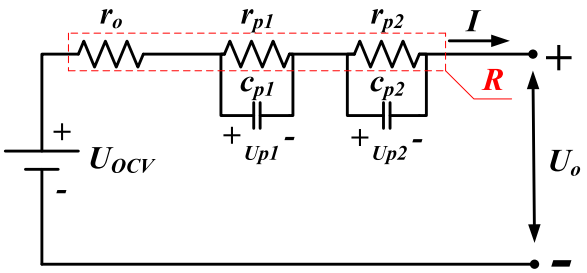


**FIGURE 1.** Schematic diagram of the 2nd-order RC model.

## II. MODEL AND OFF-LINE PARAMETER IDENTIFICATION OF LITHIUM-ION BATTERY

### A. BATTERY MODEL

The nth-order Thevenin model is widely used for SOC estimation because of its relatively high accuracy and computation efficiency compared with other models [1]. Increasing the order of the Thevenin model will improve the model accuracy further. However, higher order result in additional calculation cost [17]. In the paper, a 2nd-order RC model as shown in Fig. 1 is employed to estimate the dynamic characteristics of the battery.

The voltage source $U_{OCV}$ represents the battery OCV. $r_o$ is the internal ohmic resistance. The parallel $RC$ network consists of $r_{p1}$ and $c_{p1}$ is aimed to model the fast dynamic voltage of the battery. Similarly, the parallel $RC$ network consists of $r_{p2}$ and $c_{p2}$ is aimed to model the slow dynamic performance. $U_{p1}$ and $U_{p2}$ represent the polarization voltages across the two $RC$ networks, respectively. $U_o$ and $I$ are the terminal voltage and load current, respectively. The electrical behavior of the battery can be expressed as follows.

$$\begin{bmatrix} U_{p1}(k) \\ U_{p2}(k) \end{bmatrix} = \begin{bmatrix} e^{-\frac{T}{\tau_1}} & 0 \\ 0 & e^{-\frac{T}{\tau_2}} \end{bmatrix} \cdot \begin{bmatrix} U_{p1}(k-1) \\ U_{p2}(k-1) \end{bmatrix} + \begin{bmatrix} r_{p1} \cdot \left(1 - e^{-\frac{T}{\tau_1}}\right) \\ r_{p2} \cdot \left(1 - e^{-\frac{T}{\tau_2}}\right) \end{bmatrix} \cdot I(k) \quad (1)$$

$$U_o(k) = U_{ocv} - U_{p1}(k) - U_{p2}(k) - r_o \cdot I(k) \quad (2)$$

$$\begin{cases} \tau_1 = r_{p1} \cdot c_{p1} \\ \tau_2 = r_{p2} \cdot c_{p2} \end{cases} \quad (3)$$

where, $k$ denotes the present step, $k$-1 denotes the previous step. $T$ denotes the sampling period, $Q_N$ denotes the maximum available capacity of the battery, and $\tau_1$ and $\tau_2$ are the time constants of the RC networks. The time constants denote the response rates of $U_{p1}$ and $U_{p2}$, respectively. A higher constant means a longer time for the polarization voltage to reach balance, for a given constant load current.

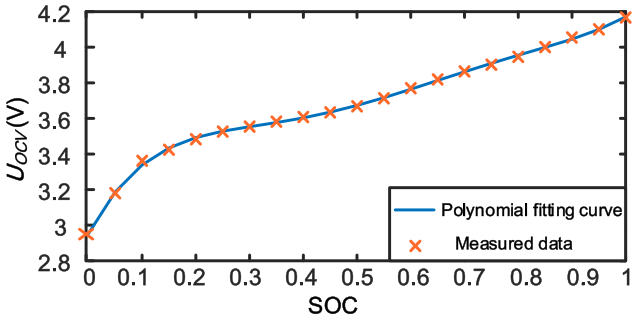


**FIGURE 2.** The offline identified SOC-OCV curve based on HPPC test.

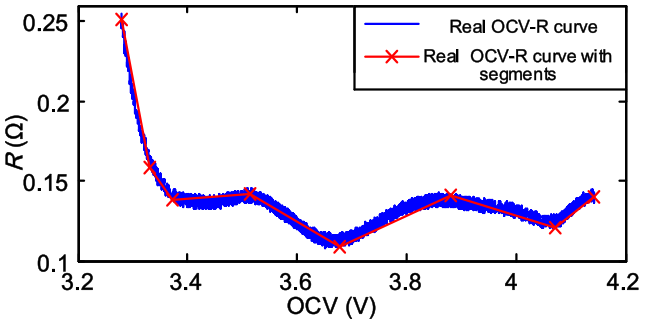


**FIGURE 3.** The offline identified OCV-R curve based on CCD test.

### B. OFF-LINE PARAMETERS IDENTIFICATION

To verify the performance of the proposed algorithm, an 18650 Li-ion battery with the nominal capacity of 3Ah and rated voltage of 3.6V was modeled. The parameter identification tests were performed on a rek-8511 programmable electronic load, where the measuring accuracy of voltage and current is 0.03%-0.05%. Then, the data were processed in Matlab. Different from the identification process in [2], the lumped resistance $R$, which is the sum of $r_o$, $r_{p1}$ and $r_{p2}$, was identified independently.

In practice, temperature and aging both have effect on battery performance. Hence, the tests were implemented under room temperature. Considering limited charging process in the test, the influence of aging on the battery performance is negligible.

#### 1) IDENTIFICATION OF SOC-OCV CURVE

The hybrid pulse power characterization (HPPC) test with one hour interval and 5% SOC each time was carried out [27].

Due to the employment of accuracy measuring equipment, the SOC could be calculated accurately based on measured data, and accuracy OCV could also be accurately measured after a long rest of the battery. The SOC-OCV relationship curve fitted by a 5-order polynomial is shown in Fig. 2.

$$U_{ocv} = 13.22SOC^5 - 39.38SOC^4 + 44SOC^3 - 22.32SOC^2 + 5.7SOC + 2.95 \quad (4)$$

#### 2) DENTIFICATION OF R-OCV CURVE

In the paper, the *R-OCV* curve will be utilized in the numerical iteration approach, which will be discussed in Section III. Hence, the identification accuracy of $R$ is critical to identify the OCV.

$$R = r_o + r_{p1} + r_{p2} \quad (5)$$

Generally, the lumped resistance $R$ defined in (5) can be calculated through the identification of $r_o$, $r_{p1}$ and $r_{p2}$, respectively. However, the curve fitting errors of $r_o$, $r_{p1}$ and $r_{p2}$ will decrease the accuracy of $R$. Therefore, the constant current discharg (CCD) test was carried out to obtain better accuracy.

During the CCD test, the battery was discharged from 100% to 10% with the discharging current of 0.8A. Consequently, the discharging process would last more than three hours. As the Li-ion battery can reach its steady state after only a few minutes [14]–[16], the transient process into steady state can be neglected compared with the whole discharging process. After the dynamic voltage enters steady state, following equation could be expressed as:

$$U_{OCV}(k) - U_o(k) = R(k) \cdot I(k) \quad (6)$$

where, $I(k)$ and $U_o(k)$ are measured based on accurate measuring instrument. Hence, $SOC(k)$ could be obtained through the CC approach. $U_{OCV}(k)$ could be calculated using the SOC-OCV curve discussed in previous Part. Then, $R(k)$ could be solved through (6). The relationship between OCV and $R$ is shown in Fig.3.

Obviously, the OCV-R curve in Fig. 3 shows strong nonlinearity. Thus it requires extremely high order polynomial to fit the curve. To simplify, the OCV-R curve is decomposed into seven linear segments according to the inflection points in the OCV-R curve. The simplified curve is expressed as the following equations:

$$R(U_{OCV}) = \begin{cases} 0.268 \cdot U_{OCV} - 0.97, & U_{OCV} \in [4.073, 4.143] \\ -0.104 \cdot U_{OCV} + 0.544, & U_{OCV} \in [3.882, 4.073] \\ 0.157 \cdot U_{OCV} - 0.468, & U_{OCV} \in [3.677, 3.882] \\ 0.201 \cdot U_{OCV} + 0.8482, & U_{OCV} \in [3.513, 3.677] \\ 0.028 \cdot U_{OCV} - 0.44, & U_{OCV} \in [3.372, 3.513] \\ -0.501 \cdot U_{OCV} + 1.827, & U_{OCV} \in [3.332, 3.372] \\ -1.744 \cdot U_{OCV} + 5.97, & U_{OCV} \in [3.278, 3.332] \end{cases} \quad (7)$$

#### 3) IDENTIFICATION OF INNER PARAMETERS:

The other inner parameters are identified based on HPPC test as well. Cooperating with the voltage response expressions [2], [28], $c_{p1}$, $c_{p2}r_o$, $r_{p1}$ and $r_{p2}$ can be obtained through curve fitting method.

$$c_{p1} = \left(-3.178SOC^4 + 8.528SOC^3 - 8.322SOC^2 + 3.311SOC - 2781\right) \cdot 10^4 \quad (8)$$

$$c_{p2} = \left(-1.015SOC^4 + 1.126SOC^3 - 4.196SOC^2 + 2.937SOC + 1124\right) \cdot 10^5 \quad (9)$$

$$r_o = 1.06SOC^5 - 3.17SOC^4 + 3.58SOC^3 - 1.84SOC^2 + 0.4SOC + 0.06 \quad (10)$$

$$r_{p1} = -4.32SOC^5 + 13.24SOC^4 - 15.28SOC^3 + 8.21SOC^2 - 2.01SOC + 0.19 \quad (11)$$

$$r_{p2} = -0.1SOC^5 - 0.05SOC^4 + 0.45SOC^3 - 0.35SOC^2 + 0.05SOC + 0.025 \quad (12)$$

## III. REAL-TIME STATE OF CHARGE ESTIMATION USING THE IMPROVED COULOMB COUNTING APPROACH

### A. STATE JUDGMENT STRATEGY FOR THE BATTERY

The principle of conventional CC approach is shown in (13). Due to the measured noise in $I$(k), an increasing accumulative error will be introduced into the SOC.

$$SOC\,(k) = SOC\,(k-1) - \frac{\eta I\,(k)\,T}{Q_N} \quad (13)$$

Generally, if the battery model is precise, model-based SOC estimation approaches, such as EKF and UKF, perform well without accumulative error. However, the accuracy of the model will be reduced at the unsteady state of a battery and model-based SOC estimation approaches have heavy calculation [16], [19], [34]. Hence, in the proposed approach, CC approach is still employed at unsteady state, and numerical iteration based on battery model is proposed to correct the SOC value at steady state. Before the proposed approach is implemented, whether the battery has been steady should be assessed.

As mentioned previously, at the steady state of a battery, the current flowing through the capacitors of the RC circuits in the model are negligible. That is to say, it can be assumed that the measured current $I$ only goes through $r_{p1}$ and $r_{p2}$. Therefore, following criterion could be formulated:

$$\begin{cases} s_1\,(k) = \dfrac{U_{p1}\,(k)}{I\,(k)\cdot r_{p1}} = 1 \\ s_2\,(k) = \dfrac{U_{p2}\,(k)}{I\,(k)\cdot r_{p2}} = 1 \end{cases} \quad (14)$$

where, $s_1$ and $s_2$ are defined as the steady coefficients, reflecting the divergence degree of the dynamic voltages from steady state. In practice, the criterion in (14) can hardly be achieved due to the complex operation condition of EVs. To address the issue, a looser criterion shown in (15) is employed. This criterion denotes that if $U_{p1}$ and $U_{p2}$ approximate to the steady state in an adjacent time domain, their mean values will also close to the steady state. Namely, the battery is in quasi-steady state. The restrictions for the mean values are aimed to eliminate the misjudgment caused by the oscillation in $I(k)$.

$$\begin{cases} \{s_1\,(k-i) \in [0.95, 1.05]\,|i = [1, 2, \cdots, n]\} \\ \{s_2\,(k-i) \in [0.95, 1.05]\,|i = [1, 2, \cdots, n]\} \\ \dfrac{\sum_{i=1}^{10} s_1\,(k-i)}{n} \in [0.95, 1.05] \\ \dfrac{\sum_{i=1}^{10} s_2\,(k-i)}{n} \in [0.95, 1.05] \end{cases} \quad (15)$$

### B. OCV ESTIMATION USING NUMERICAL ITERATION

A simple iteration algorithm is employed for OCV estimation and then the SOC could be estimated directly through SOC-OCV curve. Corresponding principle can be illustrated by (16)-(19).

$$x = \Phi\,(x) \quad (16)$$

$$x_{l+1} = \Phi\,(x_l) \quad (17)$$

$$x^* = \lim_{l\to\infty} x_{l+1} = \lim_{l\to\infty} \Phi\,(x_{l+1}) = \Phi\left(\lim_{l\to\infty} x_{l+1}\right) = \Phi\left(x^*\right) \quad (18)$$

$$x_{l+1} = x_l + \varepsilon \quad (19)$$

The equation to be solved needs to be deformed into (16) firstly, where $\Phi(x)$ is named as iterative function. Further, corresponding iteration structure can be discretized as (17), where $x_l$ is the solution of the *lth* iteration and will be taken as the input variable of the next iteration. If $x_{l+1}$ satisfies equation (18) after infinite iterations, it is treated as $x^*$, named the fixed point of $\Phi(x)$, which is the approximate solution of $x$. In practice, infinite iteration is unnecessary, and $x_l$ satisfying equation (19) is sufficient. $\varepsilon$ is a pretty small value, which is set according to the required accuracy.

Assuming that the battery is in steady state at $k$, following iteration function can be obtained.

$$U_{OCV}\,(k) = U_o\,(k) + R\,(U_{OCV}\,(k))\cdot I\,(k) \quad (20)$$

Corresponding iteration structure is shown in (21). $U_{OCV\_l}$ is the solution of the *lth* iteration, and $U_{OCV\_l+1}$ is the solution of the *(l+1)th* iteration. With iteration going on, $U_{OCV\_l+1}$ will converge to a certain value, which is the solution of $U_{OCV}(k)$. It is notable that, the initial value of $U_{OCV\_1}$ should be within the OCV range of the battery.

$$U_{OCV\_l+1} = U_o\,(k) + R\,(U_{OCV\_l})\cdot I\,(k) \quad (21)$$

Hence, given $U_o(k)$ and $I(k)$ at time $k$, the $U_{ocv}$ could be determined. To clarify the principle, an example is given in Fig. 4. In the example, $U_o(k)$ is set to be 3.2V, $I$(k) equals to 2A. Then, curve of (20) can be calculated. The initial value $U_{OCV\_1}$ is set to be 4V. In Fig.4, the arrows are used to denote the iteration process. The blue arrows start from $U_{OCV\_1}$ and end at $U_{OCV\_2}$, the red arrows start from $U_{OCV\_2}$ and end at $U_{OCV\_3}$. It is obvious that, the estimated $U_{OCV\_l}$ will finally converge to a numerical value after finite iterations, which is taken as the numerical solution of $U_{OCV}(k)$. After $U_{OCV}(k)$ is estimated, $SOC(k)$ can be precisely obtained by SOC-OCV curve without the accumulative error.

### C. COMPENSATION COEFICIENT TO PREVENT ERROR ACCUMULATION IN CC APPROACH

Assuming that numeral iteration happens at $k_i$. Then, the accumulative SOC error $E_i$ during each time interval can be calculated by following equation.

$$E_i = SOC\,(k_i) - SOC\,(k_i - 1) \quad i = 1, 2, 3\ldots \quad (22)$$

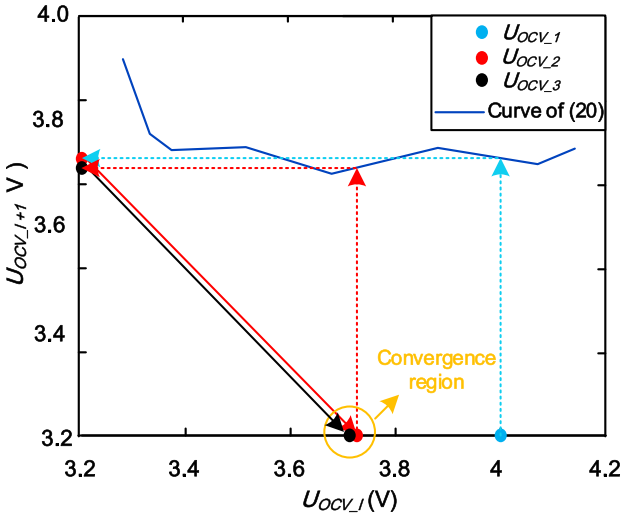


**FIGURE 4.** Convergence process of numerical iteration.

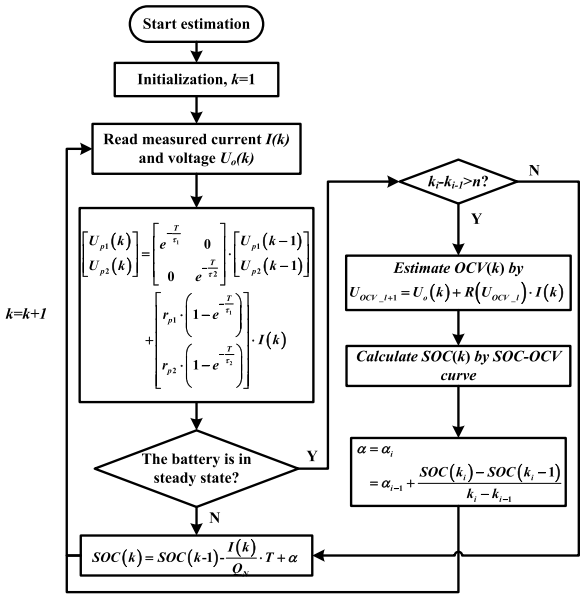


**FIGURE 5.** Flow chart of the proposed ICC approach.

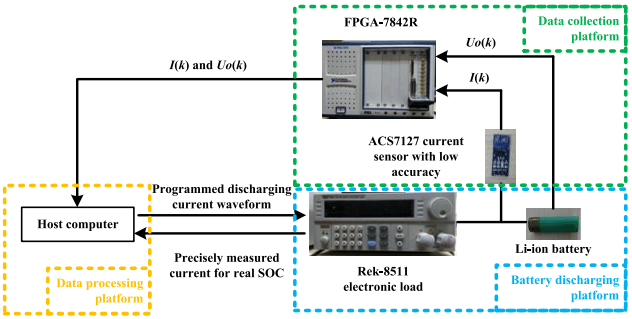


**FIGURE 6.** Block diagram of the experimental platform.

where, $SOC(k_i)$ is the precise SOC estimated by numerical iteration. $SOC(k_i-1)$ is the last SOC value got by CC, which contains the SOC error accumulated during $[k_{i-1}+1, k_i-1]$. Therefore, the error accumulation rate $\alpha$ can be estimated by following equation.

$$\alpha_i = \alpha_{i-1} + \frac{SOC\,(k_i) - SOC\,(k_i - 1)}{t_{k_i} - t_{k_{i-1}}} \tag{23}$$

where, the denominator is the time interval during $k_i$ and $k_{i-1}$, $\alpha_{i-1}$ represents the estimated accumulation rate at $k_{i-1}$, and $\alpha_i$ represents the estimated accumulation rate at $k_i$. Taking $\alpha_i$ as a compensation coefficient, the SOC estimation equation for CC approach can be improved as follows

$$SOC\,(k) = SOC\,(k-1) - \frac{I\,(k)}{Q_N} \cdot T + \alpha_i \tag{24}$$

Fig. 5 shows the flow chart of the proposed ICC approach. In Fig.5, a restrictive condition $n$ is introduced to prevent numerical iteration from occurring frequently. Considering the negligible accumulative SOC error in a short time, an interval of few minutes is suitable for each numerical iteration in practice.

## IV. EXPERIMENTAL VERIFICATION

### A. EXPRIMENTAL PLATFORM

The established experimental platform shown in Fig. 6 was utilized to verify the proposed ICC approach. The 18650 Li-ion cell, which was employed for modeling in Section II, was used in the verification experiment. The electronic load Rek-8511 was employed as discharging load. The host computer was utilized to control the discharging current of Rek-8511, while the current measured by Rek-8511 with high accuracy will be transferred to the host computer to calculate the real SOC. During the discharge process, the terminal voltage $U_o(k)$ of the cell was measured by the PXIe-7846R, a FPGA module of NI, and the current sensor ACS7127 with a low accuracy was employed to simulate the measured load current $I$ with noise in practice. Then, $I(k)$ and $U_o(k)$ were transmitted to the host computer as the input of the ICC approach. It is well known that ACS7127 is operated based on hall principle, and a current of 1A may lead a voltage output of 66mV. Correspondingly, a small error on the voltage output of ACS7127 means a relatively large error on the measured current $I$.

### B. DATA COLLECTION AND MODEL PERFORMANCE ANALYSIS

To illustrate the efficiency of the proposed ICC approach, the urban dynamometer driving schedule (UDDS) test was implemented [8]. The UDDS test lasted 4 repetitive discharging cycles. Where, the discharging current ranged from 0 to 1C-rate (3A) and the sampling period was 0.2s. During the test, 70% of the total battery charge was discharged.

Fig. 7 (a) shows the load currents measured by the electronic load Rek-8511 and the current sensor ACS7127, respectively. High frequency oscillation can be observed in $I$, it may be caused by the EMI from experimental environment. In fact, if the mean of the oscillation is zero, no error will

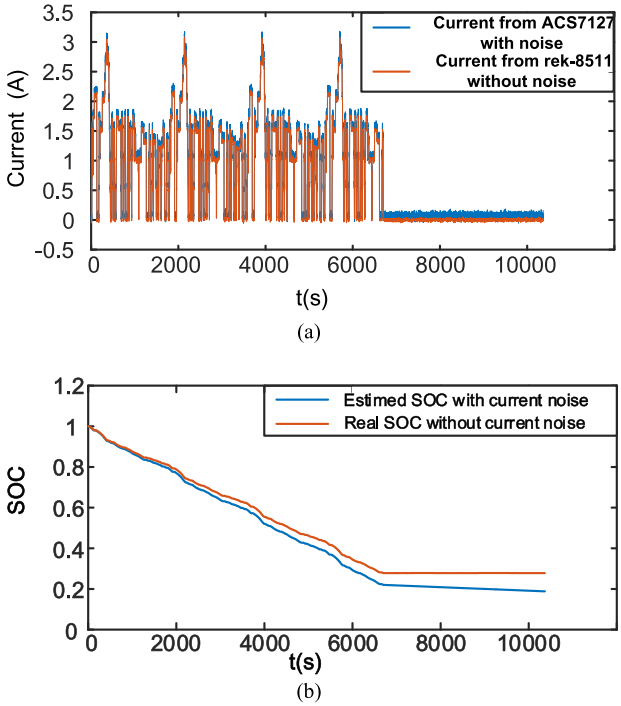


**FIGURE 7.** Measured load currents comparison between electronic load and ACS7127. (a) Measured currents. (b) Real SOC and Estimated SOC based on CC approach.

be brought into SOC for CC approach, but if the mean of the oscillation is non-zero, there will be converse result. To confirm whether the oscillation will reduce the SOC accuracy, the SOC curves estimated by CC are given in Fig. 7(b), where, the initial SOC is defined to be 1 and the estimated SOC based on the accurately measured current is defined as the real SOC. Obviously, the estimated SOC contains an increasing accumulative error. Therefore, it verified that the noise with non-zero mean is contained in the measured current $I$.

The measured and model-estimated terminal voltage curves are shown in Fig. 8 (a). The measured voltage is defined as $U_o$. In general, the proposed model can be used to estimate the battery performance well. However, there are peaks in the error curve in Fig. 8 (b). To analyze the error peaks, the zoomed-in error curve and measured current curve are shown in Fig. 8 (c). It is obvious that these error peaks are mainly caused by the current step. When the current changes relatively slow, the model performs well. Therefore, the battery model affords to identify whether the battery is at steady state.

### C. SOC ESTIMATION

Among the counterpart model-based algorithms, the EKF algorithm was taken for comparison with the proposed algorithm, considering its relatively lower computational time in each SOC estimation process.

In the paper, $n$ was set to be 100. Namely, the interval between numerical iterations was no less than 20s. The initial

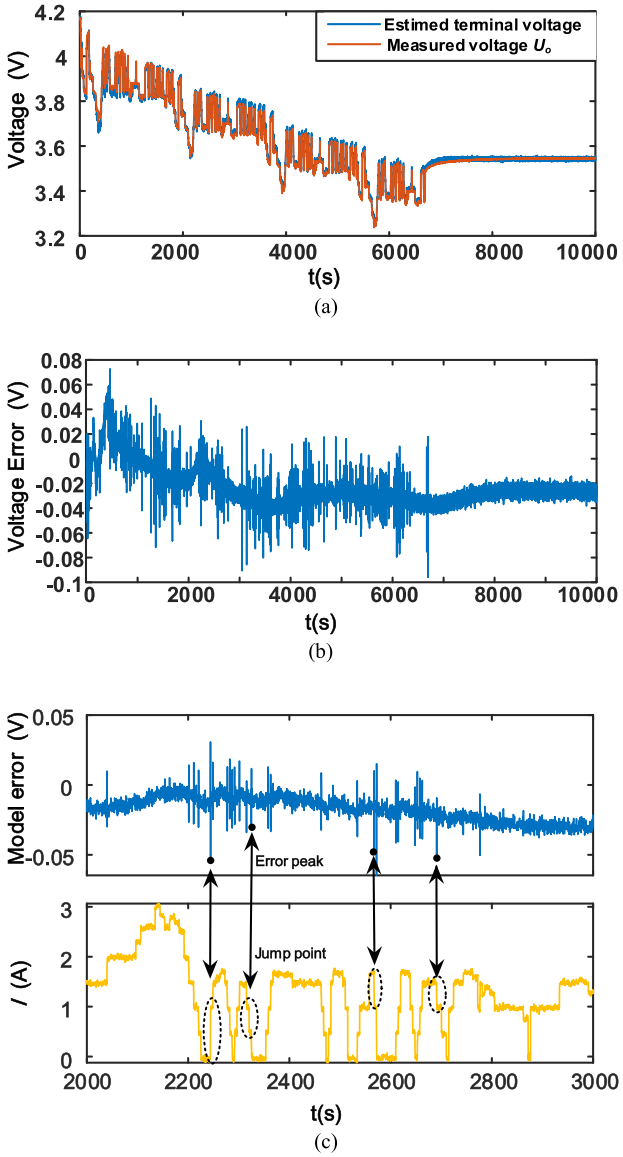


**FIGURE 8.** Terminal voltage. (a) Measured and model estimated terminal voltage. (b) Modeling error. (c) Zoom-in figures of modeling error and measured current.

value $U_{OCV\_1}$ for the numerical iteration process was set to be 3.7V. The max value of $l$ in (21) was set to be 12.

The SOC estimation curves are shown in Fig. 9. Obviously, due to the noise in the measured current $I$, the accumulated SOC error increases over time. As to EKF, it appears a weak performance with huge and oscillation error during discharging process, even though the SOC error can be corrected after the battery discharging stops. It is because only Gaussian white noise can be dealt in EKF [25]. Meanwhile, it is highly dependent on the noise statistic information [27] for EKF. The proposed ICC approach shows the best accuracy among those approaches, the SOC error in ICC approach is successfully limited to 1%. Seen from Fig.9 (b), there are many step points in the error curve based on the ICC approach. These points are where the numerical iteration occur and accumulative

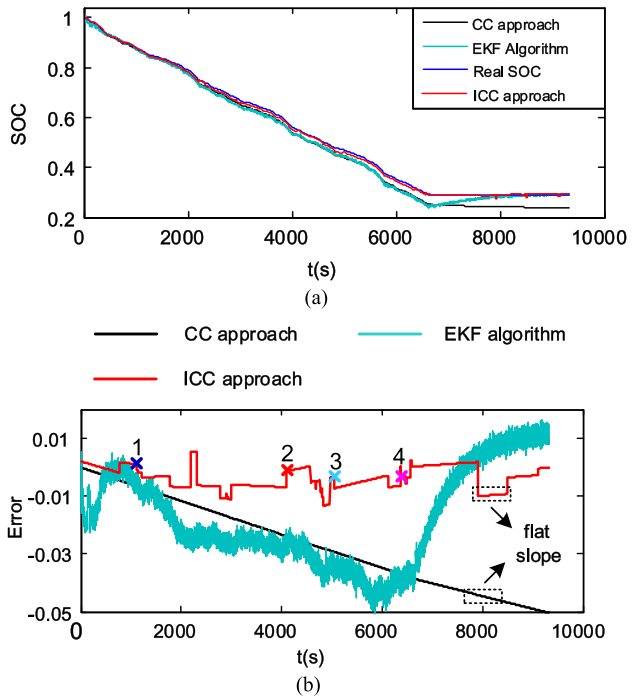


**FIGURE 9.** SOC estimation curves for UDDS. (a) SOC curve. (b) Error curves.

**TABLE 1.** Total time consumption of different algorithms under UDDS.

| Approach | Total time (s) | Average time (ms) |
|---|---|---|
| CC | 0.117 | 0.0025 |
| EKF | 23.06 | 0.494 |
| ICC | 1.328 | 0.0285 |

error is corrected. In addition, compared with traditional CC approach, the proposed ICC approach shows much slower error accumulation rate between two step points. It verifies the effectiveness of the employment of compensation coefficient $\alpha$.

To further understand the SOC estimation process based on numerical iteration, four points are selected for analysis, as marked in Fig. 9 (b).

Fig. 10 (a)-Fig.10(c) show the zoomed-in terminal voltage and the model-estimated dynamic voltages around the marked points. At each marked point, the curves of $U_{p1}$ and $U_{p2}$ are most close to the orange curves. Namely, $U_{p1}$ and $U_{p2}$ have reached to the quasi-steady state, as shown in equation (15). Fig. 10 (d) shows the numeration process at the four points. The estimated OCV value converges to a certain value after only 3 iterations in each process, suggesting an feasible calculation cost.

### D. CALCULATION COST COMPARISON

A comparison of calculation cost was performed on a 3.3GHz Intel Core i5-4590 CPU computer. The elapsed time was recorded in Matlab. Table 1 shows the results.

Seen from Table 1, the calculation time of the EKF algorithm is 197 times longer than that of the CC algorithm,

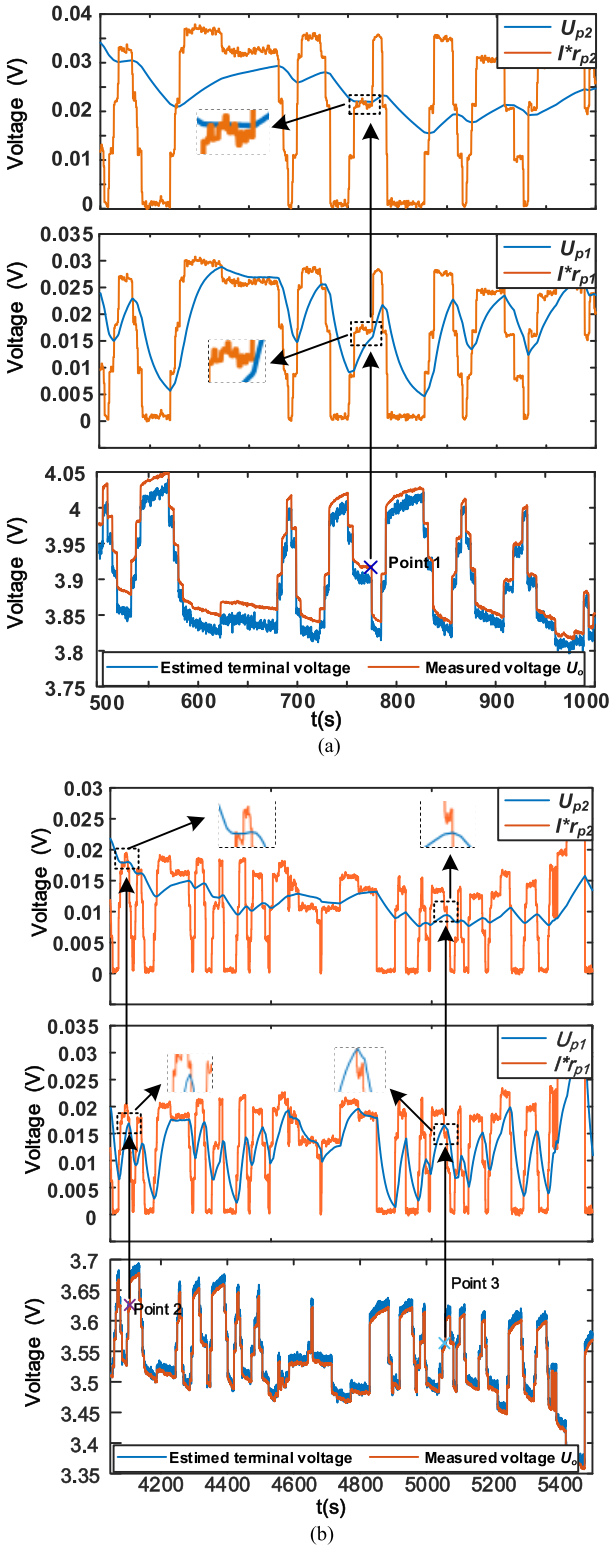


**FIGURE 10.** Details for the marked points (a)-(c) zoom-in figures of measured and model estimated terminal voltages at the marked points. (d) Numerical iteration process at the marked points.

while the proposed ICC algorithm is only 11 times longer than that of CC algorithm. Compared with EKF, about 94.4% of the calculation time is reduced in the proposed ICC approach. It is benefit for the BMS in the EV since the BMS

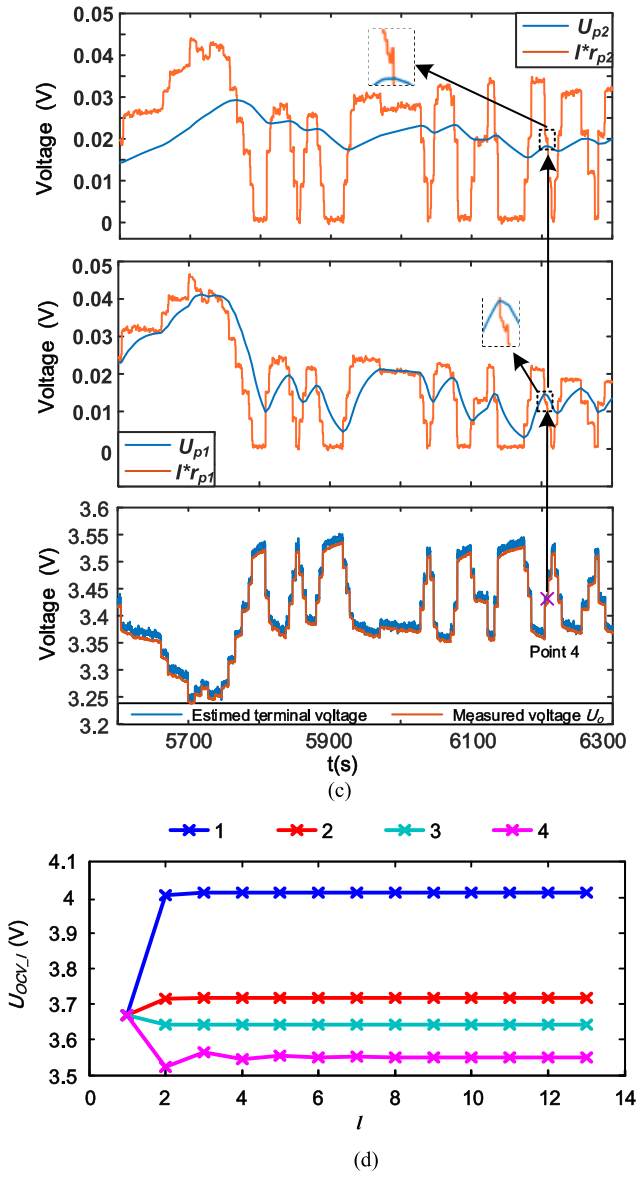


**FIGURE 10.** ***(Continued.)*** **Details for the marked points (a)-(c) zoom-in figures of measured and model estimated terminal voltages at the marked points. (d) Numerical iteration process at the marked points.**

owns much weaker calculation capability compared with the computer. Correspondingly, more computing resource can be saved for other tasks in the BMS, such as temperature control and power balance control.

## V. CONCLUSION

In the paper, an ICC approach with real-time error correction ability is proposed. The SOC is estimated online by the CC approach at unsteady state, leading a much higher estimation rate. At steady state, numerical iteration approach can accurately eliminate the accumulated SOC error of CC approach, leading a much higher accuracy than traditional CC approach. The numerical iteration approach is based on a 2nd-order RC circuit model, where its parameters were identified offline during HPPC and CCD tests. Hence, the proposed approach could combine the advantages of CC approach and model-based approach together. Furthermore, a compensation coefficient $\alpha$ is employed into the CC approach to reduce the error accumulation rate. Experimental results suggest that the SOC error of ICC is effectively limited within 1% and its calculation cost is 94% lower than that of EKF. Therefore, it provides beneficial guidance for the real-time SOC estimation in EVs.

In the future, the authors will focus on battery pack modeling under variable temperature to get accurate SOC estimation even under complex operation condition.

## REFERENCES

[1] Z. Li, J. Huang, B. Y. Liaw, and J. Zhang, "On state-of-charge determination for lithium-ion batteries," *J. Power Sources*, vol. 348, pp. 281–301, Apr. 2017.

[2] W. Yan, B. Zhang, G. Zhao, S. Tang, G. Niu, and X. Wang, "A battery management system with a lebesgue-sampling-based extended Kalman filter," *IEEE Trans. Ind. Electron.*, vol. 66, no. 4, pp. 3227–3236, Apr. 2019.

[3] C. Huang, Z. Wang, Z. Zhao, L. Wang, C. S. Lai, and D. Wang, "Robustness evaluation of extended and unscented Kalman filter for battery state of charge estimation," *IEEE Access*, vol. 6, pp. 27617–27628, 2018

[4] S. Piller, M. Perrin, and A. Jossen, "Methods for state-of-charge determination and their applications," *J. Power Sources*, vol. 96, no. 1, pp. 113–120, Jun. 2001.

[5] K. S. Ng, C.-S. Moo, Y.-P. Chen, and Y.-C. Hsieh, "Enhanced coulomb counting method for estimating state-of-charge and state-of-health of lithium-ion batteries," *Appl. Energy*, vol. 86, no. 9, pp. 1506–1511, Sep. 2009.

[6] S. G. Li, S. M. Sharkh, F. C. Walsh, and C. N. Zhang, "Energy and battery management of a plug-in series hybrid electric vehicle using fuzzy logic," *IEEE Trans. Veh. Technol.*, vol. 60, no. 8, pp. 3571–3585, Oct. 2011.

[7] J. Chen, O. Ouyang, C. Xu, and H. Su, "Neural network-based state of charge observer design for lithium-ion batteries," *IEEE Trans. Control Syst. Technol.*, vol. 26, no. 1, pp. 313–320, Jan. 2018.

[8] E. Chemali, P. J. Kollmeyer, M. Preindl, R. Ahmed, and A. Emadi, "Long short-term memory networks for accurate state-of-charge estimation of Li-ion batteries," *IEEE Trans. Ind. Electron.*, vol. 65, no. 8, pp. 6730–6739, Aug. 2018.

[9] G. O. Sahinoglu, M. Pajovic, Z. Sahinoglu, Y. Wang, P. V. Orlik, and T. Wada, "Battery state-of-charge estimation based on regular/recurrent Gaussian process regression," *IEEE Trans. Ind. Electron.*, vol. 65, no. 5, pp. 4311–4321, May 2018.

[10] H. Chaoui and C. C. Ibe-Ekeocha, "State of charge and state of health estimation for lithium batteries using recurrent neural networks," *IEEE Trans. Veh. Technol.*, vol. 66, no. 10, pp. 8773–8783, Oct. 2017.

[11] L. Lu, X. Han, J. Li, J. Hua, and M. Ouyang, "A review on the key issues for lithium-ion battery management in electric vehicles," *J. Power Sources*, vol. 226, pp. 272–288, Mar. 2013.

[12] X. Hu, S. Li, and H. Peng, "A comparative study of equivalent circuit models for Li-ion batteries," *J. Power Sources*, vol. 198, pp. 359–367, Jan. 2012.

[13] J. Yang, B. Xia, Y. Shang, W. Huang, and C. C. Mi, "Adaptive state-of-charge estimation based on a split battery model for electric vehicle applications," *IEEE Trans. Veh. Technol.*, vol. 66, no. 12, pp. 10889–10898, Dec. 2017.

[14] Z. Wei, T. M. Lim, M. Skyllas-Kazacos, N. Wai, and K. J. Tseng, "Online state of charge and model parameter co-estimation based on a novel multi-timescale estimator for vanadium redox flow battery," *Appl. Energy*, vol. 172, pp. 169–179, Jun. 2016.

[15] H. Dai, T. Xu, L. Zhu, X. Wei, and Z. Sun, "Adaptive model parameter identification for large capacity Li-ion batteries on separated time scales," *Appl. Energy*, vol. 184, pp. 119–131, Dec. 2016.

[16] A. Hentunen, T. Lehmuspelto, and J. Suomela, "Time-domain parameter extraction method for Thévenin-equivalent circuit battery models," *IEEE Trans. Energy Convers.*, vol. 29, no. 3, pp. 558–566, Sep. 2014.

[17] Z. Wei, C. Zou, F. Leng, B. H. Soong, and K.-J. Tseng, "Online model identification and state-of-charge estimate for lithium-ion battery with a recursive total least squares-based observer," *IEEE Trans. Ind. Electron.*, vol. 65, no. 2, pp. 1336–1346, Feb. 2018.

[18] R. Xiong, H. He, and K. Zhao, "Research on an online identification algorithm for a Thevenin battery model by an experimental approach," *Int. J. Green Energy*, vol. 12, no. 3, pp. 272–278, Oct. 2014.
[19] C. Zhang, K. Li, J. Deng, and S. Song, "Improved realtime state-of-charge estimation of $LiFePO_4$ battery based on a novel thermoelectric model," *IEEE Trans. Ind. Electron.*, vol. 64, no. 1, pp. 654–663, Jan. 2017.
[20] B. Xiong, J. Zhao, Y. Su, Z. Wei, and M. Skyllas-Kazacos, "State of charge estimation of vanadium redox flow battery based on sliding mode observer and dynamic model including capacity fading factor," *IEEE Trans. Sustain. Energy*, vol. 8, no. 4, pp. 1658–1667, Oct. 2017.
[21] Z. Liu, G. Sun, S. Bu, J. Han, X. Tang, and M. Pecht, "Particle learning framework for estimating the remaining useful life of lithium-ion batteries," *IEEE Trans. Instrum. Meas.*, vol. 66, no. 2, pp. 280–293, Feb. 2017.
[22] C. Lin, H. Mu, R. Xiong, and W. Shen, "A novel multi-model probability battery state of charge estimation approach for electric vehicles using H-infinity algorithm," *Appl. Energy*, vol. 166, pp. 76–83, Mar. 2016.
[23] W. Wang, S. Yang, C. Lin, and Y. Li, "State of charge dependent constitutive model of the jellyroll of cylindrical lithium-ion cells," *IEEE Access*, vol. 6, pp. 26358–26366, 2018.
[24] L. Zheng, L. Zhang, J. Zhu, G. Wang, and J. Jiang, "Co-estimation of state-of-charge, capacity and resistance for lithium-ion batteries based on a high-fidelity electrochemical model," *Appl. Energy*, vol. 180, pp. 424–434, Oct. 2016.
[25] R. Xiong, H. He, F. Sun, and K. Zhao, "Evaluation on state of charge estimation of batteries with adaptive extended Kalman filter by experiment approach," *IEEE Trans. Veh. Technol.*, vol. 62, no. 1, pp. 108–117, Jan. 2013.
[26] J. Han, D. Kim, and M. Sunwoo, "State-of-charge estimation of lead-acid batteries using an adaptive extended Kalman filter," *J. Power Sources*, vol. 188, no. 2, pp. 606–612, Mar. 2009.
[27] H. He, R. Xiong, X. Zhang, F. Sun, and J. Fan, "State-of-charge estimation of the lithium-ion battery using an adaptive extended Kalman filter based on an improved Thevenin model," *IEEE Trans. Veh. Technol.*, vol. 60, no. 4, pp. 1461–1469, May 2011.
[28] Z.-L. Zhang, X. Cheng, Z.-Y. Lu, and D.-J. Gu, "SOC estimation of lithium-ion batteries with AEKF and wavelet transform matrix," *IEEE Trans. Power Electron.*, vol. 32, no. 10, pp. 7626–7634, Oct. 2017.
[29] D. Andre, C. Appel, T. Soczka-Guth, and D. U. Sauer, "Advanced mathematical methods of SOC and SOH estimation for lithium-ion batteries," *J. Power Sources*, vol. 224, pp. 20–27, Feb. 2013.
[30] P. Shen, M. Ouyang, L. Lu, J. Li, and X. Feng, "The co-estimation of state of charge, state of health, and state of function for lithium-ion batteries in electric vehicles," *IEEE Trans. Veh. Technol.*, vol. 67, no. 1, pp. 92–103, Jan. 2018.
[31] C. Chen, R. Xiong, and W. Shen, "A lithium-ion battery-in-the-loop approach to test and validate multiscale dual H infinity filters for state-of-charge and capacity estimation," *IEEE Trans. Power Electron.*, vol. 33, no. 1, pp. 332–342, Jan. 2018.
[32] S. Muhammad, M. U. Rafique, S. Li, Z. Shao, Q. Wang, and N. Guan, "A Robust algorithm for state-of-charge estimation with gain optimization," *IEEE Trans. Ind. Informat.*, vol. 13, no. 6, pp. 2983–2994, Dec. 2017.
[33] M. Paschero, G. L. Storti, A. Rizzi, F. M. F. Mascioli, and G. Rizzoni, "A novel mechanical analogy-based battery model for SoC estimation using a multicell EKF," *IEEE Trans. Sustain. Energy*, vol. 7, no. 4, pp. 1695–1702, Oct. 2016.
[34] Q. Zhu, L. Li, X. Hu, N. Xiong, and G.-D. Hu, "$H_\infty$-based nonlinear observer design for state of charge estimation of lithium-ion battery with polynomial parameters," *IEEE Trans. Veh. Technol.*, vol. 66, no. 12, pp. 10853–10865, Dec. 2017.

**LIANGZONG HE** was born in Hunan, China, in 1984. He received the B.Sc. degree from Jilin University, Changchun, China, in 2006, and the Ph.D. degree from the Huazhong University of Science and Technology, Wuhan, China, in 2012. From 2009 to 2011, he was a joint Ph.D. education student with Michigan State University, East Lansing, MI, USA. In 2012, he joined Xiamen University, Xiamen, China, as an Assistant Professor, and has been an Associate Professor since 2015. His research interests include dc-dc converters, switched capacitor converters, Z-source converters, wireless power transmission, and microgrid.

**DONG GUO** received the B.E. degree from Qinghai University, Xining, China, in 2015. He is currently pursuing the Ph.D. degree with the Department of Power Electronics, Xiamen University, Xiamen, China. His research interests include battery management system in electric vehicles and wireless power transfer.